REGIONAL CLIMATIC MODELS OF WIND AND TEMPERATURE ALTITUDE DISTRIBUTIONS IN THE ATMOSPHERIC BOUNDARY LAYER

V.S. Komarov, V.I. Akselevich, A.V. Kreminskii, and N.Ya. Lomakina

Institute of Atmospheric Optics,
Siberian Branch of the Russian Academy of Sciences, Tomsk
Russian State Institute for Hydrometeorology, St. Petersburg
Received June 28, 1995

We discuss here some results of applied statistical simulation of the altitude distributions of wind and temperature in the boundary layer of the atmosphere. The simulation is intended for constructing regional climate models and estimating air pollution level over local areas.

Among numerous problems on climate and ecology monitoring over local areas, an important one is the statistical simulation of altitude structure of meteorological fields (of temperature and wind, first of all) in the atmospheric boundary layer (with top at 1–2 km) by making use of data of long-standing aerological observations. Such an importance is because the temperature and wind regime in the boundary layer are major contributors to the mesoclimate change (typically at scales on the order of hundreds of meters horizontally and near one thousand meters vertically[1,2]). In addition, this factor can affect the mesoclimate indirectly, by altering the level of air pollution and the rate of changes, this influences the atmospheric optical and radiation properties and thus the mesoclimate itself. The effect of temperature and wind regime on the pollution level and its variation is well described by the transfer equation for anthropogenic pollution, which for a particular impurity in the turbulent atmosphere is written as

$$\frac{\partial s}{\partial t} = -\left(u\frac{\partial s}{\partial x} + v\frac{\partial s}{\partial y}\right) - w\frac{\partial s}{\partial z} - \frac{\partial w_a s}{\partial z} + k_s\left(\frac{\partial^2_s}{\partial x^2} + \frac{\partial^2_s}{\partial y^2}\right) + \\ + \frac{\partial}{\partial z}k_z\frac{\partial s}{\partial z} - \varepsilon_a, \qquad (1)$$

where s is the concentration of the impurity a; t is the time; u, v, and w are the wind velocity components along x, y, and z coordinates; k_s and k_z are the coefficients of atmospheric circulation in horizontal and vertical planes, respectively; w_a is the impurity vertical velocity; and $\varepsilon_a = \varepsilon_a(x, y, z, t)$ is the impurity source (sink), i.e., its generation (dissipation) rate per unit volume.

Indeed, from the equation we can see that the primary factor driving the impurity spread from the source is the advective impurity inflow (first term on the right-hand side of the equation), which is determined by the values of latitudinal (u) and longitudinal (v) wind components, and the impurity inflow due to vertical turbulent exchange (fourth term on the right-hand side of the equation) whose effectiveness strongly depends on temperature stratification (via Richardson criterion).

It should be emphasized here that most of the gaseous and solid pollutants important to mesoclimate and coming from soil spread mostly within the boundary layer, i.e., well below 1.5 to 2 km.

All this demonstrates a great need in climate modeling for incorporating altitude distribution of temperature and wind within atmospheric boundary layer. In addition to climate models for free atmosphere being widely used in applied geophysics (see, e.g., Refs. 4–7), the models of interest here have not received due attention so far.

Taking all the above, the authors have attempted to create regional climate models incorporating vertical wind and temperature distributions within the atmospheric boundary layer (up to a height of 2 km).

This paper presents some results of our studies of two typical regional models. The models are based on data of long–term (1961–1978) observations at two stations, L'vov (49°49' N, 23°51' E) and Novosibirsk (55°02' N, 82°54' E), representative of two quasihomogeneous regions in the Northern hemisphere as identified in the course of objective classification of climate types.[6] All in all about 2000 observations were used to construct each of the regional climate models. The models employed certain grid of geometric altitudes as vertical coordinates. The observations are presented by data at specific points and isobaric surfaces, so linear interpolation was applied to observations to obtain data at selected altitudes. For geometric levels we took station altitude h_0 and the heights 0.1, 0.2, 0.3, 0.4, 0.6, 0.8, 1.2, 1.6, and 2.0 km.

Regional statistical models of temperature and wind in the boundary layer built upon long–term data include: (a) vertical profiles of the mean values $\overline{\xi}(h_i)$ and standard (rms) deviations $\sigma_\xi(h_i)$ of temperature (T°,C), latitudinal (u, m/s) and longitudinal (v, m/s) components of wind velocity (below we shall call them latitudinal and longitudinal winds); (b) autocorrelation matrices $\|R_{\xi\xi}\|$ of these parameters, as well as the profiles of the maximum (ξ_{max}) and minimum (ξ_{min}) values of medium-term variables $\xi_{short\text{-}term}(h_i)$ inferred from short–term observations and allowing the amplitude of the diurnal

0235-6880/95/12 1044-08 $02.00

behavior of $\overline{\xi}_{\text{short–term}}$, that is the difference $\xi_{max} - \xi_{min,}$ (Ref. 8) to be estimated at various levels in the atmospheric boundary layer.

Let us now discuss in more detail the constructed statistical models of the vertical distributions of temperature and wind velocity components.

MODELS OF VERTICAL TEMPERATURE DISTRIBUTION

The main features of regional statistical models of the vertical temperature distribution constructed for boundary layer are summarized in Table I in terms of the profiles of $\overline{T}$ and $\sigma_{\overline{T}}$ as well as correlation matrix $\|R_{\overline{T}\overline{T}}\|$ all calculated for winter and summer seasons, and in Fig. 1 showing examples of the altitude distributions of $\overline{T}$, T_{max}, and T_{min} typical of the models constructed.

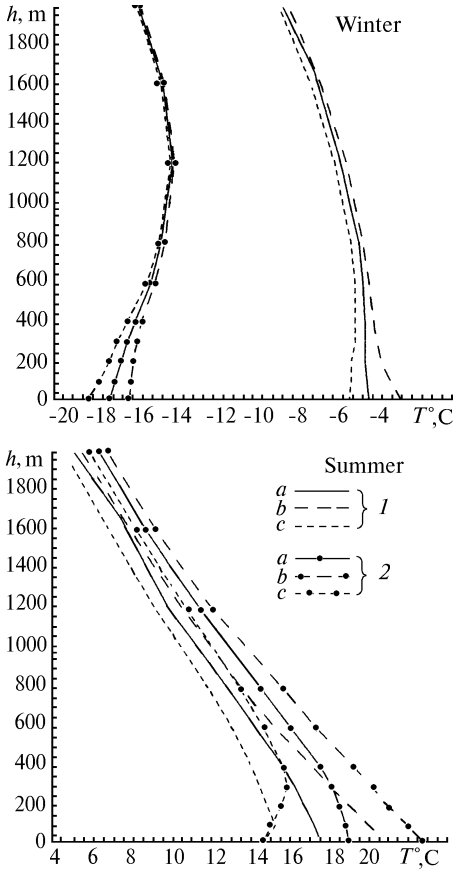

FIG. 1. Model profiles of altitude distribution of the mean (a), maximum (b), and minimum (c) values of temperature for the first (1) and second (2) quasihomogeneous regions.

From Table I and Fig. 1 as well as from other data available we obtain that the model altitude profiles of $\overline{T}$ and $\sigma_{\overline{T}}$ in the boundary layer show a distinct dependence on season, geographic location of the quasihomogeneous region, and on the time of a day. Specifically:

(1) In winter the altitude distributions of the mean temperature in both models have a segment with temperature nearly constant or varying inversely up to high altitudes (800 m in the first model and 1200 m in the second), while in summer both models produce nearly identical distributions with $\overline{T}$ decreasing up to the boundary layer top.

(2) The mean temperature calculated from short–term observations shows a distinct diurnal behavior, however, most pronounced in summer, in which season the diurnal amplitude of $\overline{T}_{\text{short-term}}$ varies from 6.7° near ground to 0.9° at 800 m (in the first model), and from 8.5° near ground to 0.9° at 2000 km (in the second model). In winter the marked diurnal temperature variations with an about 0.7° to 2.7° amplitude are observed mostly in the boundary layer bottom (600 m thick layer in the first model and 300 m thick layer in the second).

(3) The vertical profiles of rms deviation of temperature $\sigma_{\overline{T}}$ for the two regional models are substantially different in winter but very much similar in summer. Thus, in particular, in the first model the value of $\sigma_{\overline{T}}$ is practically constant throughout the boundary layer, while in the second model its value decreases with altitude in winter, but both model values of $\sigma_{\overline{T}}$ in summer decrease with altitude up to 2 km.

(4) Unlike the mean temperature, its rms deviation calculated over finite time periods shows no diurnal variation except at three lower levels (0, 100, and 200 m) whose $\Delta\sigma = \sigma_{max} - \sigma_{min}$ value of 0.8° to 1.4° is well above the temperature measurement error of 0.7° below 5 km altitude.[9]

Complete description of the temperature models being constructed must also include specific interlevel correlations inherent in each quasihomogeneous region under consideration. Let us use for this purpose temperature autocorrelation matrices $\|R_{\overline{T}\overline{T}}\|$ also presented in Table I.

Analysis of all the model matrices obtained has revealed same features specific to the boundary atmospheric layer, in addition to known relations of the interlevel correlations such as their weakening with increasing interlayer distance. The specific features are as follows:

(a) both regional models typically have marked seasonal distinctions in vertical behavior of the interlevel correlation coefficients $r_{\overline{T}\overline{T}}(h_i, h_j)$ whose winter values fall off faster (with decreasing distance between correlated levels) than summer values in the most part of the layer (up to 800 m altitude).

(b) in winter the correlation coefficients between temperature variations at the station level (or 100 m and 200 m altitudes as in the first model) and temperature variations at all the above-lying levels typically exhibit transition through the extremum of $r = 0.6$, i.e., through the lower boundary of the region of high correlation (in summer such a transition of $\gamma_{\overline{T}\overline{T}}(h_i, h_j)$ through $r = 0.6$ does not take place).

TABLE I. Regional statistical models of the temperature profiles.

Height, m	Model No. 1									
	Height, m									
	0	100	200	300	400	600	800	1200	1600	2000
	$\overline{T}$,°C									
	-4.2	-4.3	-4.4	-4.4	-4.4	-4.5	-4.7	-5.6	-6.9	-8.5
	$\sigma_{\overline{T}}$,°C									
	5.5	5.5	5.7	5.8	5.7	5.5	5.5	5.6	5.7	5.8
										Winter
0	1.000	0.971	0.914	0.859	0.821	0.747	0.679	0.579	0.518	0.482
100	0.968	1.000	0.976	0.933	0.895	0.818	0.745	0.640	0.574	0.536
200	0.915	0.978	1.000	0.979	0.948	0.873	0.799	0.690	0.623	0.584
300	0.877	0.951	0.984	1.000	0.985	0.920	0.847	0.739	0.672	0.631
400	0.856	0.931	0.969	0.989	1.000	0.957	0.888	0.782	0.714	0.672
600	0.826	0.899	0.939	0.965	0.981	1.000	0.967	0.870	0.798	0.752
800	0.792	0.866	0.907	0.935	0.957	0.984	1.000	0.934	0.863	0.815
1200	0.726	0.795	0.836	0.867	0.895	0.936	0.967	1.000	0.954	0.908
1600	0.688	0.751	0.788	0.819	0.846	0.890	0.925	0.968	1.000	0.971
2000	0.658	0.716	0.747	0.773	0.797	0.837	0.870	0.915	0.959	1.000
	Summer									
	$\overline{T}$,°C									
	17.6	17.2	16.7	16.2	15.6	14.2	12.8	9.8	7.3	4.9
	$\sigma_{\overline{T}}$,°C									
	4.4	4.2	4.1	4.1	4.0	3.8	3.7	3.6	3.5	3.4
	Model No. 2									
	Height, m									
	0	100	200	300	400	600	800	1200	1600	2000
	$\overline{T}$,°C									
	-17.2	-16.9	-16.6	-16.3	-15.9	-15.1	-14.6	-14.0	-14.5	-15.7
	$\sigma_{\overline{T}}$,°C									
	9.2	8.7	8.4	8.1	7.9	7.5	7.1	6.5	6.3	6.2
										Winter
0	1.000	0.969	0.935	0.895	0.864	0.803	0.742	0.613	0.568	0.565
100	0.976	1.000	0.985	0.957	0.932	0.877	0.820	0.698	0.648	0.639
200	0.920	0.977	1.000	0.988	0.970	0.922	0.869	0.749	0.696	0.684
300	0.864	0.941	0.984	1.000	0.992	0.955	0.905	0.785	0.730	0.718
400	0.825	0.909	0.963	0.989	1.000	0.978	0.936	0.819	0.764	0.750
600	0.775	0.865	0.927	0.964	0.984	1.000	0.980	0.878	0.822	0.804
800	0.746	0.837	0.901	0.940	0.964	0.987	1.000	0.932	0.876	0.853
1200	0.670	0.762	0.827	0.868	0.896	0.928	0.961	1.000	0.954	0.921
1600	0.639	0.727	0.791	0.832	0.859	0.890	0.925	0.968	1.000	0.975
2000	0.624	0.707	0.768	0.806	0.832	0.859	0.889	0.927	0.968	1.000
	Summer									
	$\overline{T}$,°C									
	19.0	18.8	18.5	18.1	17.5	16.0	14.5	11.4	8.6	6.2
	$\sigma_{\overline{T}}$,°C									
	5.1	4.8	4.6	4.5	4.5	4.4	4.3	4.2	4.2	4.0

Moreover, analysis of the autocorrelation matrices $\|R_{\overline{T}\overline{T}}\|_{\text{short–term}}$ obtained for isolated periods (too cumbersome to be reproduced here) shows that diurnal behavior has only little effect on the behavior of interlevel correlation coefficients of temperature in the boundary layer except for the correlation between this meteorological value at the station level (or 100 m and 200 m altitudes as in the first model) and its values at all levels above.

MODELS OF ALTITUDE DISTRIBUTION OF LATITUDINAL WIND

Main features of these models are seen from Table II composed of the parameters $\overline{U}$, $\sigma_{\overline{U}}$, and $\|R_{\overline{U}\overline{U}}\|$, and from Fig. 2 exemplifying model profiles $\overline{U}(h)$, $U_{\max}(h)$, and $U_{\min}(h)$. Analysis of Table II and Fig. 2 shows that altitude distributions of U and σ_U, like those of T and σ_T, have marked dependence on season, location and the type of diurnal behavior, which, however, are somewhat different from those of temperature profiles.

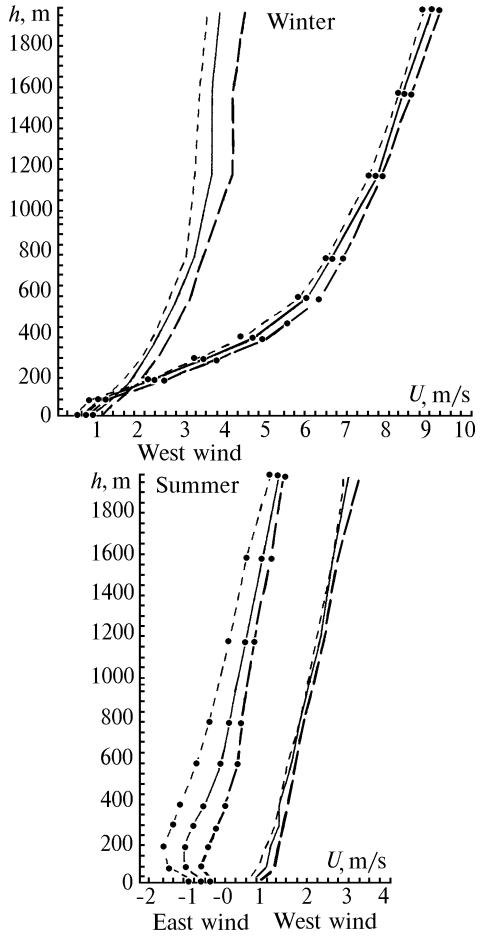

FIG. 2. Model profiles of altitude distribution of the mean (a), maximum (b), and minimum (c) values of latitudinal wind velocity for the first (1) and second (2) quasi–homogeneous regions (see Fig. 1 for designations).

First, unlike to the model profiles of altitude distribution of the mean temperature, $\overline{T}(h)$, analogous profiles for the mean latitudinal wind speed $\overline{U}$ show spatial stability in winter (in which season the regional models of latitudinal wind are both characterized not only by the same western latitudinal winds but also by its acceleration with altitude throughout the boundary layer), while exhibiting strong spatial variability in summer; specifically while first model in this season has the same western wind increasing in velocity up to 2 km altitude, characteristic of the second model are weak eastern wind dominating up to 600 m altitude, its turning to the west near 600 m to increase and dominate in the above layers of the boundary layer.

Second, similar seasonal variation (like that of $\overline{U}$) also occurs in vertical distribution of standard deviation $\sigma_{\overline{U}}$; specifically, this parameter typically behaves similarly throughout the boundary layer in both models in winter, but the models have different $\sigma_{\overline{U}}$ profiles in summer, when $\sigma_{\overline{U}}$ steadily grows with altitude, though not as rapidly as it does in winter, in the first model, while in the second model, $\sigma_{\overline{U}}$ increases with altitude from a value at the station level to a maximum at 600 m, goes through a marked minimum, and then continues to grow with altitude up to the boundary layer top.

Third, for mean latitudinal wind velocity calculated from short-term data, as for the temperature, it is characteristic that marked diurnal behavior is observed (standard deviation $\sigma_{\overline{U}}$ does), but, in contrast to temperature, it possesses a more complex character of amplitude variation with altitude, and regional peculiarities in annual behavior (while in the first Cuasi–homogeneous region (station L'vov) the largest amplitude of diurnal behavior of $\overline{U}$ (of the order of 0.4–1 m/s) is observed in winter and the minimum (less than 0.3 m/s) in summer, the second Cuasi–homogeneous region (station Novosibirsk) shows an inverse pattern, with the largest values (0.6–1.1 m/s) in summer and the smallest (less than 0.5 m/s) in winter.

The interlevel correlations of latitudinal wind velocity were analyzed in terms of autocorrelation matrices $\|R_{\overline{U}\overline{U}}\|$ (see Table II), as well as the matrices $\|R_{\overline{U}\overline{U}}\|$ (not presented in the paper), and they were shown to be weaker than temperature correlations with the only feature characteristics, namely, the dependence of the two Cuasi–homogeneous regions. Thus, in the first model $r_{\overline{U}\overline{U}}(h_i, h_j)$ values decrease slowly with distance between the correlated levels in all seasons, while in the second model these correlations decrease more rapidly, so that interlevel correlation coefficients between latitudinal wind velocity values at the near-ground layer and all the above layers are less than 0.6 already at 400 m in winter and 800 m in summer.

TABLE II. Regional statistical models of latitudinal wind velocity profiles.

Height, m	Model No. 1									
	Height, m									
	0	100	200	300	400	600	800	1200	1600	2000
	$\overline{U}$, m/s									
	0.7	1.3	1.8	2.1	2.4	2.9	3.3	3.7	3.7	3.9
	$\sigma_{\overline{U}}$, m/s									
	2.7	4.0	4.9	5.4	5.8	6.3	6.7	7.5	7.5	7.7
									Winter	
0	1.000	0.908	0.856	0.835	0.804	0.746	0.702	0.622	0.597	0.564
100	0.877	1.000	0.954	0.928	0.895	0.829	0.771	0.674	0.639	0.603
200	0.831	0.957	1.000	0.977	0.945	0.880	0.825	0.726	0.685	0.645
300	0.813	0.936	0.980	1.000	0.985	0.934	0.882	0.786	0.747	0.705
400	0.787	0.901	0.948	0.984	1.000	0.968	0.921	0.829	0.791	0.748
600	0.738	0.838	0.887	0.941	0.973	1.000	0.974	0.899	0.859	0.810
800	0.700	0.788	0.839	0.895	0.931	0.976	1.000	0.954	0.912	0.859
1200	0.618	0.681	0.727	0.784	0.820	0.889	0.950	1.000	0.966	0.910
1600	0.582	0.642	0.684	0.741	0.777	0.846	0.907	0.962	1.000	0.968
2000	0.543	0.603	0.643	0.696	0.728	0.793	0.849	0.904	0.973	1.00
	Summer									
	$\overline{U}$, m/s									
	0.6	1.1	1.2	1.4	1.4	1.7	1.9	2.4	2.7	3.1
	$\sigma_{\overline{U}}$, m/s									
	1.9	3.0	3.5	3.8	4.0	4.4	4.6	5.2	5.3	5.5
	Model No. 2									
	Height, m									
	0	100	200	300	400	600	800	1200	1600	2000
	$\overline{U}$, m/s									
	0.5	1.0	2.3	3.5	4.7	6.0	6.6	7.7	8.3	9.0
	$\sigma_{\overline{U}}$, m/s									
	2.2	4.5	5.6	6.1	6.7	7.4	7.5	7.9	8.2	8.5
									Winter	
0	1.000	0.779	0.660	0.626	0.579	0.531	0.527	0.498	0.499	0.492
100	0.726	1.000	0.868	0.834	0.781	0.721	0.710	0.660	0.652	0.623
200	0.659	0.870	1.000	0.964	0.907	0.837	0.816	0.745	0.731	0.701
300	0.660	0.855	0.968	1.000	0.977	0.928	0.902	0.815	0.797	0.767
400	0.646	0.815	0.913	0.978	1.000	0.976	0.946	0.851	0.831	0.800
600	0.615	0.756	0.834	0.925	0.973	1.000	0.982	0.896	0.871	0.840
800	0.596	0.729	0.793	0.883	0.932	0.975	1.000	0.948	0.919	0.885
1200	0.518	0.619	0.651	0.727	0.767	0.835	0.918	1.000	0.963	0.924
1600	0.497	0.593	0.621	0.691	0.727	0.792	0.877	0.967	1.000	0.975
2000	0.479	0.563	0.590	0.656	0.689	0.750	0.831	0.917	0.973	1.000
	Summer									
	$\overline{U}$, m/s									
	−0.2	−0.9	−0.9	−0.7	−0.4	0	0.2	0.6	1.0	1.4
	$\sigma_{\overline{U}}$, m/s									
	1.8	3.2	4.1	4.2	4.3	4.5	4.4	4.6	4.8	4.9

MODELS OF ALTITUDE DISTRIBUTION OF THE LONGITUDINAL WIND

To fully understand specific features of regional models describing the vertical statistical structure of longitudinal wind field in the boundary layer of individual Cuasi–homogeneous regions, let us refer now to Tables III and Fig. 3 for an illustration examples of altitude distributions of $\overline{V}$, V_{max}, and V_{min}.

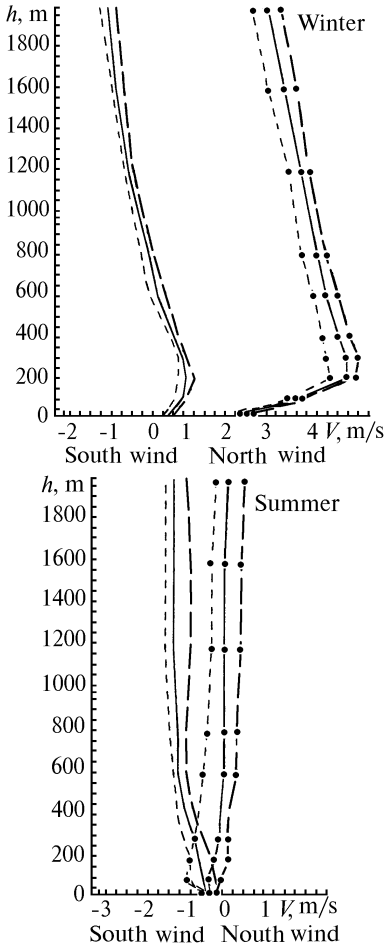

FIG. 3. Model profiles of altitude distribution of the mean (a), maximum (b), and minimum (c) values of longitudinal wind for the first (1) and second (2) quasi–homogeneous regions (see Fig. 1 for designations).

Upon examination of Table III and Fig. 3, as well as other relevant materials one can see that the statistical models of altitude distribution of longitudinal wind also possess specific features, namely:

– both Cuasi–homogeneous regions being considered are typically dominated by northern winds in winter and southern winds in summer, with the total number of layers dominated by these winds being dependent on the model. In winter the northern winds flow in 0–90 m layer in the first model, while dominating the entire boundary layer in the second. At the same time, in summer when the southern winds dominate over the entire boundary layer in the first model, while being restricted to its bottom (up to 600 m altitude) in the second model, the situation is Cuite opposite;

– the altitude profiles of longitudinal wind velocity, $\overline{V}(h_i)$, differ much more substantially in winter than in summer. Specifically, in winter the first model is characterized by larger longitudinal wind velocity and the presence of a more pronounced maximum in V behavior at 200–300 m altitudes. Unlike, the summer two models differ only a little in the profiles of altitude distribution of longitudinal wind velocity;

– mean longitudinal wind velocities compiled for isolated periods, like latitudinal winds, have certain diurnal behavior (undetectable only in winter in the first Cuasi–homogeneous region) being, however, essentially different from that of latitudinal wind (cf. Figs. 2 and 3). Thus, if in winter marked amplitudes of the diurnal behavior of $\overline{V}_{short\text{-}term}$, as large as 0.6–0.8 m/s, occurring between 200 and 2000 m are typical for the second model and not for the first (as it was for latitudinal wind), in summer marked amplitude of diurnal behavior of $\overline{V}_{short\text{-}term}$ (of 0.3 to 0.8 m/s) are now typical for both models (a feature typical of the second model only in the case of latitudinal wind);

– altitude distribution of $\sigma_{\overline{V}}$ obtained for boundary layer of the two separated Cuasi–homogeneous regions shows close similarity in that the value $\sigma_{\overline{V}}$ in both seasons is almost the same (at all levels) and behaves analogously with altitude (grows) up to the layer top;

– standard deviations of the longitudinal wind velocity calculated for some periods mostly have no diurnal behavior except in summer for the first model when almost everywhere in the boundary layer (except for station level) an increased amplitude (on the order of 0.8–1 m/s) of diurnal behavior of $\sigma_{\overline{V}}$ is observed with the value exceeding the standard error in radiosonde measurements of wind velocity components whose value is 0.7 m/s at altitudes lower than 10 km at $V \le 10$ m/s (Ref. 9),

– interlevel correlation coefficients in both models $r_{\overline{V}\overline{V}}(h_i, h_j)$ behave with altitude similarly in winter, in summer being different in the case of latitudinal wind. In particular, in winter the correlation coefficients $r_{\overline{V}\overline{V}}$ (0...300 m) decrease with level separation slower in the first model than in the second (as in the case of correlation coefficients of latitudinal wind), while in summer both models show similar behaviors (decelerated decrease) of interlevel correlation coefficients $r_{\overline{V}\overline{V}}(h_i, h_j)$ with altitude, whose values taken between latitudinal wind velocity values at station level and all the above layers, that is, $r_{\overline{V}\overline{V}}(h_0, h_i)$, typically pass through $r = 0.6$ near 1000 m altitude, which is not characteristic of $r_{\overline{U}\overline{U}}(h_0, h_i)$ coefficients.

TABLE III. Regional statistical models of longitudinal wind profiles

Height, m	Model No. 1									
	Height, m									
	0	100	200	300	400	600	800	1200	1600	2000
	$\overline{V}$, m/s									
	0.5	0.9	1.0	0.9	0.7	0.3	0.1	−0.4	−0.7	−0.9
	$\sigma_{\overline{V}}$, m/s									
	2.3	3.7	4.4	4.7	5	5.5	5.9	6.6	6.8	7.2
	Winter									
0	1.000	0.906	0.864	0.839	0.802	0.741	0.688	0.616	0.580	0.539
100	0.880	1.000	0.954	0.924	0.878	0.804	0.738	0.656	0.619	0.577
200	0.830	0.954	1.000	0.974	0.931	0.860	0.795	0.710	0.671	0.626
300	0.808	0.926	0.977	1.000	0.980	0.923	0.861	0.773	0.731	0.683
400	0.775	0.884	0.940	0.982	1.000	0.963	0.906	0.819	0.775	0.723
600	0.722	0.815	0.873	0.934	0.971	1.000	0.970	0.893	0.844	0.787
800	0.678	0.759	0.816	0.880	0.920	0.972	1.000	0.950	0.895	0.837
1200	0.564	0.619	0.670	0.732	0.774	0.857	0.937	1.000	0.961	0.902
1600	0.513	0.565	0.607	0.667	0.708	0.790	0.873	0.948	1.000	0.971
2000	0.474	0.517	0.549	0.605	0.642	0.718	0.796	0.871	0.968	1.000
	Summer									
	$\overline{V}$, m/s									
	−0.4	−0.5	−0.6	−0.7	−0.9	−1.1	−1.1	−1.2	−1.2	−1.2
	$\sigma_{\overline{V}}$, m/s									
	1.8	3.0	3.4	3.7	3.9	4.2	4.3	4.9	4.9	5.2
	Model No. 2									
	Height, m									
	0	100	200	300	400	600	800	1200	1600	2000
	$\overline{V}$, m/s									
	2.0	3.7	4.9	4.9	4.7	4.4	4.2	3.8	3.4	3.0
	$\sigma_{\overline{V}}$, m/s									
	2.7	4.4	5.6	5.6	5.8	6.0	6.0	6.1	6.4	6.7
	Winter									
0	1.000	0.787	0.703	0.687	0.656	0.607	0.578	0.490	0.467	0.445
100	0.759	1.000	0.906	0.874	0.819	0.738	0.702	0.603	0.567	0.525
200	0.708	0.925	1.000	0.966	0.907	0.813	0.764	0.654	0.615	0.572
300	0.704	0.908	0.976	1.000	0.976	0.908	0.858	0.740	0.700	0.657
400	0.689	0.871	0.936	0.983	1.000	0.962	0.914	0.790	0.750	0.707
600	0.664	0.819	0.877	0.941	0.976	1.000	0.974	0.862	0.820	0.779
800	0.647	0.788	0.843	0.905	0.940	0.979	1.000	0.927	0.881	0.836
1200	0.566	0.666	0.712	0.763	0.794	0.855	0.929	1.000	0.950	0.898
1600	0.525	0.615	0.658	0.706	0.738	0.802	0.879	0.961	1.000	0.970
2000	0.485	0.572	0.610	0.656	0.685	0.746	0.823	0.905	0.971	1.000
	Summer									
	$\overline{V}$, m/s									
	−0.2	−0.4	−0.2	−0.1	−0.1	0	0	0	0	0.1
	$\sigma_{\overline{V}}$, m/s									
	1.8	3.5	4.3	4.5	4.7	4.8	4.6	4.7	4.9	5.1

Summarizing, it should be emphasized that the results obtained here complement and justify data on modeled distribution of temperature and wind in free atmosphere. Their extension to the entire northern hemisphere, however, reQuires construction of new regional models of altitude distribution of temperature and wind in the boundary layer, and will be the subject of our future studies.

REFERENCES

1. K.Ya. Kondratiev, *Global Climate,* Itogi Nauki i Tekhniki, Ser. Meteorologia i Gidrologia (Moscow, 1987), 313 pp.
2. O.A. Drozdov, et al., *Climatology* (Gidrometeoizdat, Leningrad, 1989), 567 pp.
3. P.N. Belov and V.S. Komarov, Atmos. Oceanic Opt. **7**, No. 2, 103–107 (1994).
4. C.C. Justus, et al., *Four I. Global Reference Atmospheric Technical Rescription,* Part 1, NASA US C–TMX–64871, Sept. 1974.
5. V.E. Zuev and V.S. Komarov, *Statistical Models of the Temperature and Gaseous Components of the Atmosphere* (D. Reidel Publishing Company, Dordreht, Boston–Lancaster–Tokyo, 1987), 306 pp.
6. V.S. Komarov and V.A. Remenson, Opt. Atm. **1**, No. 7, 3–16 (1988).
7. V.S. Komarov and V.A. Remenson, Atmos. Oceanic Opt. **8**, No. 5, 386–390 (1995).
8. L.T. Matveev, *Course of the General Meteorology. Atmospheric Physics* (Gidrometeoizdat, Leningrad, 1984), 751 pp.
9. V.D. Reshetov, Tr. Tsentr. Aerol. Obs., No. 133, 55–65 (1978).